encit 2020

ABCM Associação Brasileira de Engenharia e Ciências Mecânicas

18th Brazilian Congress of Thermal Sciences and Engineering
November 16-20, 2020 (Online)

ENC-2020-0603
Development of natural convection solar drying system

Rodrigo Eduardo Predolin
Vicente Luiz Scalon
Geraldo Luiz Palma
São Paulo State University (UNESP), School of Engineering, Bauru
spg.feb@unesp.br

Abstract. *Most foods deteriorate very easily, to minimize this problem, some food preservation techniques have emerged, among which, drying is one of the most used. The advantages of drying food are better preservation of the product, reduction of its weight, with the consequent reduction in the cost of transportation and storage. With drying, decreasing the amount of water, not only the weight decreased, but it also creates unfavorable conditions for the microbial growth of the product. An indirect solar dryer with natural convection was developed, constructed and experimentally investigated. It is formed for 3 main parts: absorber plate with 0.5 m^2 area of surface, dryer chamber and exhaust duct, highlighting that the absorbed plate has the possibility modify it's position and direct the flow air that was initially over the upper face, to the upper and lower face (double passage). This change increased the moisture removal rate from 0.47 g/min to 0.56 g/min, the total moisture removal from 185 g to 220 g and the average daily thermal efficiency from 8.5% to 19.8%. The analysis of the equipment was possible due to the presence of temperature, humidity and atmospheric pressure sensors positioned at air inlet and outlet, a turbine type anemometer at the air outlet, 3 temperature sensors and the cell load located in the drying chamber, allowing to record moisture removal, which can also be calculated by mass balance with the data provided by sensors at the entrance and exit of air in the dryer system.*
Keywords: *Indirect solar dryer, Solar absorber panel, Convective solar dryer.*

1. INTRODUCTION

Processing food for storage usually requires its water removal. Depending on the method used, it can be very expensive in energy consumption or impair in the food quality or its properties. An alternative to food dehydration is the use of solar energy, one of the oldest techniques for food preservation. The food drying using solar energy can occur in an open environment with solar radiation using direct contact with the food (direct solar dryer). It also can be done in an environment insulated from solar radiation (indirect solar dryer) using the air heated by a solar radiation absorber plate. In this case, the heated airflow into a chamber where food is stored and the water is removed by mass transfer.

Several studies evaluating solar dryers can be found in the literature. Rajkumar *et al.* (2007), for example, analyze the drying kinetics of sliced tomatoes in a vacuum solar dryer and comparing with the data obtained in an open solar dryer over the climatic conditions of Montreal, Canada. Based on the results obtained, it was verified that when the temperature in the vacuum chamber reaches 18 °C over the environmental temperature, the drying time of the products for obtaining 11.5% humidity (wet basis), was 20% lower if compared to the open solar dryer. The author highlights the product quality obtained in this case based on the low oxidation, color and flavor preservation.

Another controlled study is developed by Singh and Kumar (2012) in an indoor environment using typical solar dryers (direct and indirect, with and without forced ventilation). Several tests were made to obtain the convection heat transfer coefficient for these models using different air velocities. Changes in incident energy from the radiant source over the absorber plate are simulated using electrical heaters. The study provided, in addition to the heat transfer coefficient, a summary analysis for the main physical parameters of the equipment.

An experimental investigation was also developed by Mohajer *et al.* (2013) using a hybrid system for heating water and for supplying hot air to a food dryer. The device is similar to the models usual for heating residential water with a modified solar collector. In this case, there are triangular section ducts below the absorber plate for air circulation and they are connected to the drying chamber. The analysis was performed with forced airflow of 0.021 kg/s and waterflow of 0.001 kg/s. Two different configurations were analyzed: with and without the air heating by electric resistance assistance. The results shows that the use of the auxiliary electric heater increases the air temperature in the drying chamber in about 20 to 30 °C above to the one that uses solar energy only. The auxiliary heater increased temperature to close to 56 °C and interfered in the food quality. However, the use of a hybrid model implied in a cost reduction and occupied space of about 49% if compared to independent water and air heating systems.

Baniasadi *et al.* (2017) analyzed a mixed solar dryer with forced air circulation and a thermal storage system. The results shows that the drying rate remained almost constant throughout the day. This behaviour can be explained by the

use of the stored solar energy in the absorber plate. This change in air dryer device increased the thermal efficiency in about 11% and drying efficiency for apricot food in 10%.

This paper aims to evaluate an indirect solar dryer, as shown in fig. 2, designed and built to allow several changes in its components. The effectiviness of design changes are evaluated comparing the results obtained by original design with the modified ones in the same operational conditions. The equipment was mounted and installed in the city of Bauru, Brazil, with latitude 22°21'S longitude 49°02'W. The analysis of the equipment was developed from October to December 2019 (spring and summer). This study evaluates the influence in changing the absorber flat plate position for solar dryer over several parameters like airflow, drying effects, considering the water evaporation and changes in air moisture, and other ones.

2. Materials and methods

The used solar dryer was assembled using a profiled steel structure, insulating material (EPS) of 35 mm thickness, glass plate of 3 mm thickness and electronic components that form sensoring and data storage system. All the instruments and sensors were assembled for this test using the Arduino open platform. Different kinds of sensors for humid air and load cells were tested to obtain better results. Figure 1 shows the main parts of the mounted solar dryer:

1. Absorbier plate: black metallic surface with measurements 0.5m x 1m (0.5 m^2), covered with commercial glass of 3 mm thickness and away from the plate at most 0.1 m;
2. Lower drying chamber: in order to make broad analysis of the equipment, it was designed to allow two regions of food dehydration;
3. Upper drying chamber: usual food dehydration region in similar equipment;
4. Exhaust duct for heated air, with cross-section measurements of 0.25 m x 0.5 m (0.125 m^2) and maximum height in relation to the ground 2.4 m.

Figure 1. indirect solar dryer photography:(1) absorber plate, (2) e (3) drying chamber, (4) exhaust duct.

The air flow inside the equipment occurs by natural convection due to the heating of the absorber plate using two possible configurations as shown in fig. 2. The first configuration uses the absorber plate positioned near the insulated bottom surface. In this arrangement, the airflow occurs only on the upper surface, which is far from the cover glass in 100 mm. The second configuration uses the plate in a midrange position and allows the air flow on both surfaces. Despite the lower surface is not exposed to solar radiation as the upper surface, the heat conduction process also increases its temperature. In this absorber position, the plate is 50 mm far from the cover glass.

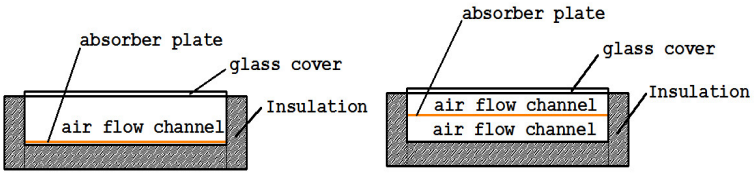

Figure 2. Absorbent plate configuration: (a) configuration 1: plate insulated on the bottom surface with air flow on up surface; (b) configuration 2: with air flow on both surfaces of the absorber plate.

2.1 Instrumentation

Several sensors were installed in specific regions of the the solar dryer to characterize its physical behavior. The installed sensors are used for measuring humidity, temperature, atmospheric pressure, load cell and flow sensor. Better description for the installed sensors and its positions inside the equipment are presented for the seven regions shown in fig. 3:

- Region 1: Lower part of the equipment, atmospheric air inlet, in this region there are 2 sensors, the sensor *BME280*, Bosch Sensor manufacturer, capable of measuring atmospheric pressure, air temperature and relative humidity of the inlet air. The second sensor is dedicated to temperature measurement, identified as *DS18b20*, Maxim Integrated manufacturer;
- Region 2: Region where the absorber plate is located and on the underside of this plate (region not exposed to solar radiation), there are 3 temperature sensors (*DS18b20*) installed along its length, thus determining its temperature profile;
- Region 3: Thermal radiometer, Avallone *et al.* (2018), positioned beside to the equipment with the same absorber plate inclination;
- Region 4: Load cell with capacity from 0 to 2000 g, used to determine the evaporation rate, and another *DS18b20* temperature sensor;
- Region 5: Heated air outlet duct, upper region, where there are the same sensors as region 1, that is, *BME280* relative humidity and pressure sensor, and the *DS18b20* sensor, that is responsible for obtaining only the outlet air temperature;
- Region 6: Exit end of the heated air, where there is the turbine-type anemometer;
- Região 7: Insulated location where the *datalogger* is located, responsible for recording all sensor information.

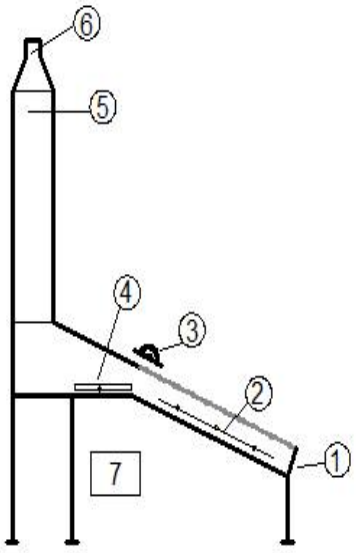

Figure 3. Sketch identifying the region where the sensors are located.

The equipment was configured to evaluate the solar dryer thermal performance and obtain the evaporation rate for the two configurations of absorber plate previous described. The tests were runned from 10:00AM and 5:00PM, with the equipment loaded with water in a container with an exposed wet area from 0.132 m^2.

2.2 Formulation

The operation of the dryer depends on some important parameters and directly measured by the sensors, such as: air flow, absorber plate temperature, incident solar radiation, air temperature externally and internally to the dryer. Other parameters depends on calculations which are performed using the data provided by the sensors postprocessed by the Coolprop software Bell *et al.* (2014), such as: enthalpy, absolute humidity and air density.

Instantaneous thermal efficiency is defined as the relationship between the useful energy (Q_u) and the incident solar radiation (G_t) on the tilted absorbent plate (A_c):

$$\eta = Q_u / A_c.G_t \tag{1}$$

where the useful energy is obtained by the difference in enthalpy of the incoming humid air (h_{in}) and outlet humid air (h_{out}):

$$Q_u = (h_{out} - h_{in}) \cdot \dot{m} \tag{2}$$

where the air enthalpy is evaluated using the humidity sensor data and processed by the Coolprop software using the HAPropsSI function. The average mass flow of humid air $\dot{m}$ is obtained by the equation:

$$\dot{m} = \rho \cdot u_{air} \cdot S \tag{3}$$

where ρ is the density of the heated humid air, u_{air} is the average speed of the humid heated air at the dryer outlet (location 6, fig. 3) e S is the area of the turbine-type anemometer.

3. Results and discussions

The indirect solar dryer was tested in two different positions for the absorber plate: configuration 1 and 2, as shown in fig. 2. The results of these configuration changes were compared and analyzed for a day test. The climatic conditions for the test days in which were performed both configurations were similar, as well as the solar irradiation. In the test day of configuration 1 the average solar radiation was 613 W/m^2 and the total daily incident solar radiation was 15.67 MJ/m^2. In the test day for configuration 2, the average solar radiation was 613 W/m^2 and the total daily incident solar radiation was 15.84 MJ/m^2.

The first analysis evaluates the influence of the plate position, changed from configuration 1 to configuration 2, on the air flow. This design change results in increase of averaged mass flow values from 4.17 g/s to 4.4 g/s, an equivalent increase of 5.5 %. As indicated in fig. 4, the air flow is also more stable in configuration 2, presenting small ocilations with variations in incident radiation if compared to configuration 1.

The temperature profile of the absorber plate was analyzed by the presence of three temperature sensors, the first one is positioned close to the external air inlet, the second one is located at a half of the plate length and the third, is positioned at the end of the plate length. Using these sensors it was possible to observe the increase in the plate temperature over the environmental temperature ($T_{plate} - T_{enviroment}$) due to the incident radiation. For configurations 1 and 2, the lower region of the plate, close to the external air entrance remains lower than the other regions. This effect can be explained by the cold ambient air on heat exchange as observed in fig. 5. For other temperature sensor positions, higher temperatures were verified for both configurations. However for configuration 2 the board are about 5 °C colder than configuration 1, with the lower position temperature values changed from 58 °C to 53 °C and the central part of the absorber plate the change was from 71,5 °C to 67 °C, indicating improvement in natural convection in configuration 2.

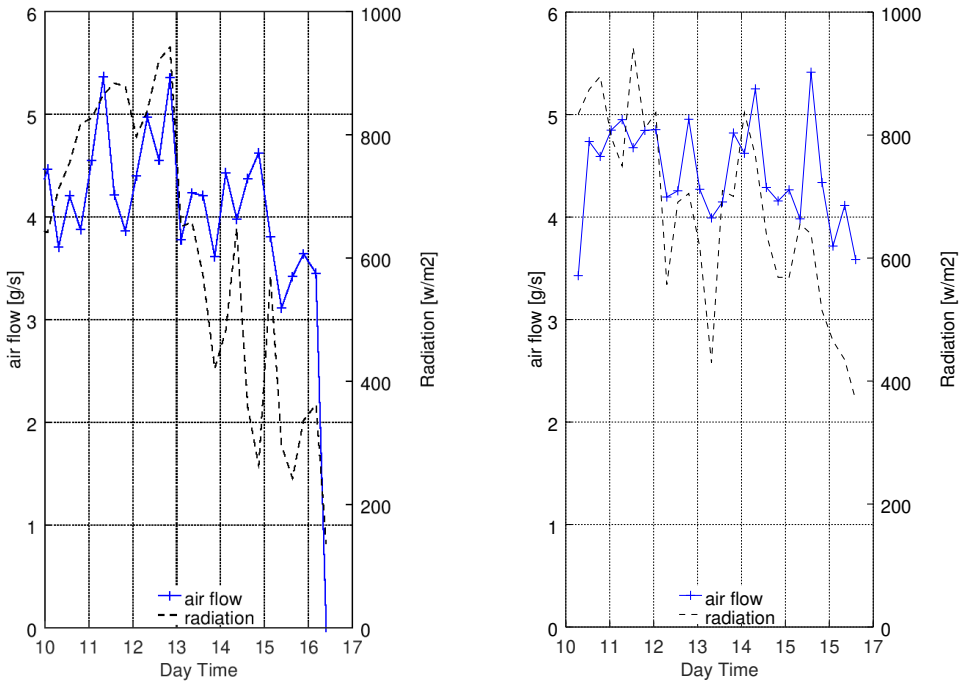

Figure 4. Hot air flow in the indirect solar collector. (a) configuration 1, absorber plate lower position, (b) configuration 2, raised absorber plate.

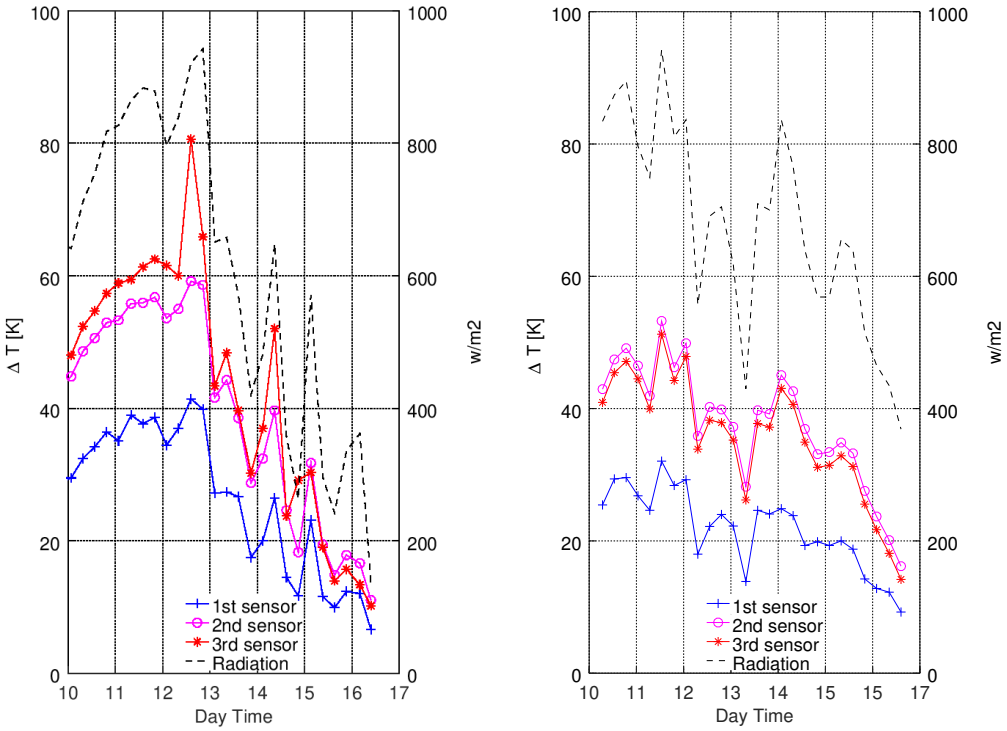

Figure 5. Temperature difference between the absorber plate and the environment. (a) configuration 1, (b) configuration 2.

The temperature difference between outlet and inlet air is greater on the configuration 2 for absorber plate, as seen in fig. 6. One can observe that the increase in the air temperature flowing through dryer was greater and more stable in

configuration 2, resulting in 7.3 °C average throughout the day and maximum of 11.7 °C. For the same analisys, it is observed an averaged temperature increase of 3 °C on configuration 1, with maximum value of 4.9 °C.

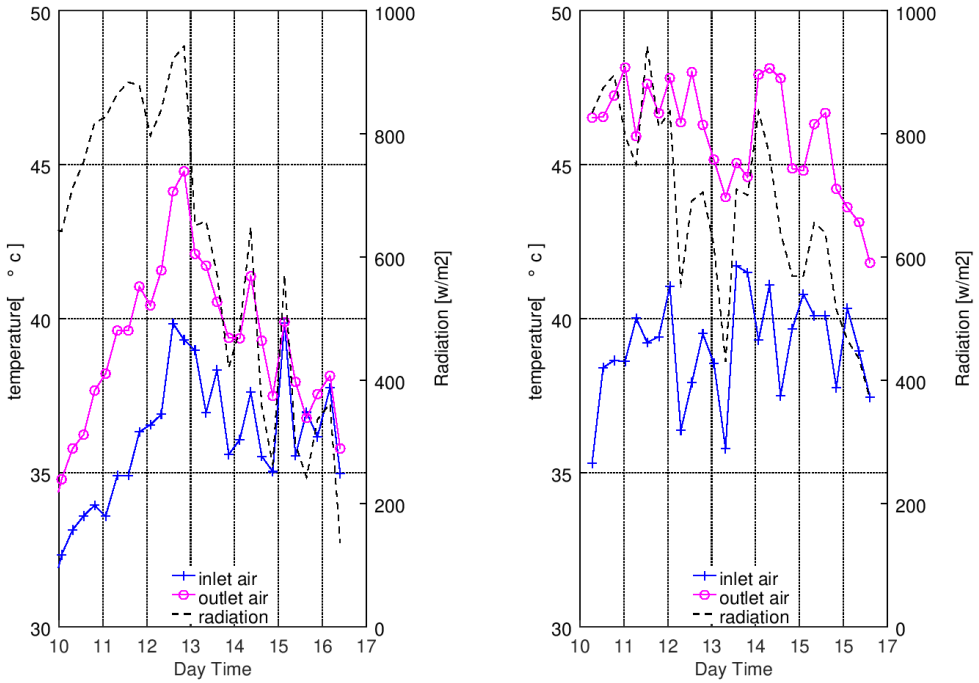

Figure 6. inlet air temperature in the dryer and outlet air temperature in the dryer. (a) configuration 1, (b) configuration 2.

The relative humidity at the inlet and outlet air in the dryer can be mapped due to the presence of humidity sensors at the entrance and exit of the equipment. The fig. 7 shows these values for configuration 2 indicating that the outlet air is less humid in relation to the inlet air than in configuration 1. This is a great advantage for drying devices. By other hand, the average difference daily in relative humidity between the inlet and outlet air for configuration 1 is 3.3% and for configuration 2 is 6%.

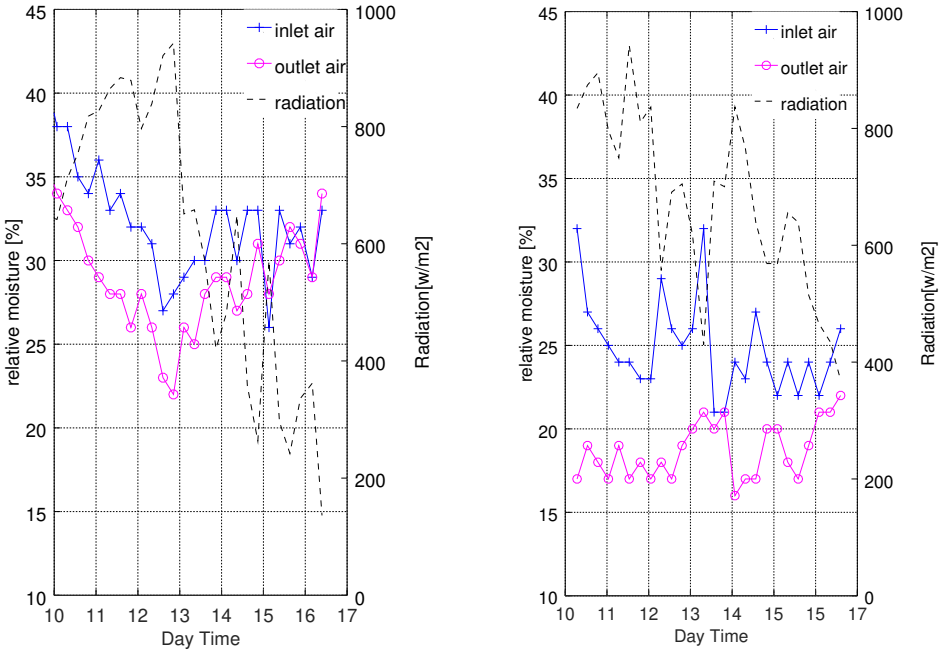

Figure 7. Relative humidity at the entrance of the dryer and relative humidity at the exit of the dryer. (a) configuration 1, (b) configuration 2.

Considering the data obtained for temperature, atmospheric pressure and relative humidity sensors at the entrance and exit of the dryer, associated with air mass flow inside the equipment, it was possible to determine the quantitative of moisture removed along the day. Using the sensor data, it is possible evaluate this parameter by two different methods. The first method was performed using the load cell located in the drying chamber, which reports the amount of water removed from the reservoir at 15 minute intervals. The second method is performed using the difference in absolute humidity for the outlet air in relationship with the inlet air (obtained with the aid of the Coolprop software), multiplied by the average flow in the computed interval.

These two methods are compared and presented in fig. 8 and fig. 9. According these presented values, there is a significant variation in the amount of water removed durind the day obtained by method 1 and 2 (load cell and absolute humidity, fig. 8a). This difference can be explained by oscillations in the air flow, as noted in fig. 4, once the flow data are recorded only at 15 minute intervals. Variations in flow during this time interval are not recorded, therefore, if the air flow is constant, the results obtained by the moisture difference method will be better. This can be noted in configuration 2 of the absorber plate which provides more constant flow if compared to configuration 1. In this configuration, the estimative of the removed water is closed for the both methods, as seen in the graph to the right of fig. 8. Analyzing the data related to the moisture removed as function of position on the absorber plate, one can conclude that configuration 2 promoves better water removal values then the configuration 1.

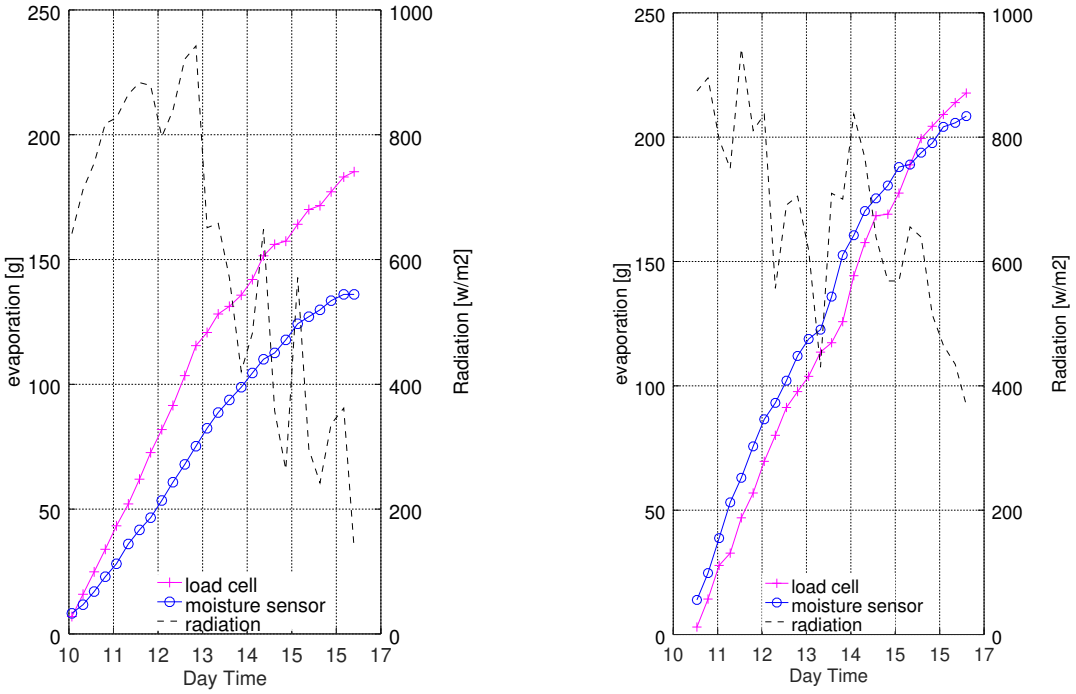

Figure 8. Amount of water removed during the day (accumulated), by the method of absolute humidity difference and the load cell record, with registration every 15 minutes. (a) configuration 1, (b) configuration 2.

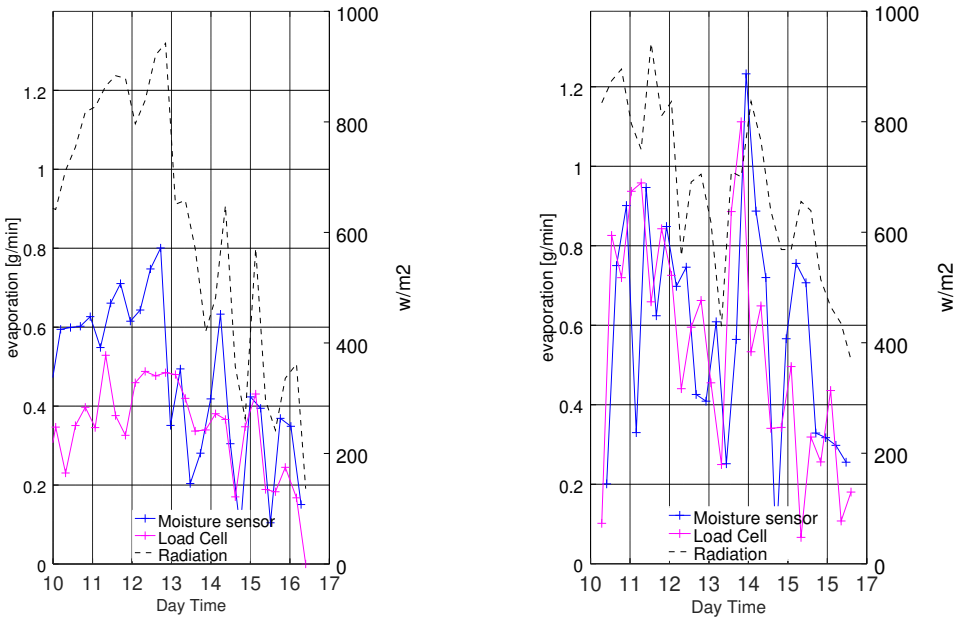

Figure 9. Amount of water removed every 15 minutes, by the method of absolute humidity difference and the load cell record, with registration every 15 minutes. (a) configuration 1, (b) configuration 2.

Using the data provided by the sensors at the entrance and exit of the equipment (humidity, temperature and atmospheric pressure sensors), the calculation of the enthalpy of the humid air at the entrance and exit of the equipment is performed, with this, the thermal efficiency of the equipment in function of the incident solar radiation is determined, as shown in fig. 10, having superior thermal efficiency for configuration 2, with average daily values of 19.8 % and for configuration 1 the value obtained was 8,4 %.

Figure 10. average thermal efficiency of the equipment every 15 minutes depending on the incident solar radiation. (a) configuration 1, (b) configuration 2.

4. CONCLUTION

This study developed an experimental test of an indirect solar dryer with based on the uses of several sensors, making it possible to obtain the main thermal characteristics of solar dryer. Considering the two configurations evaluated for the absorber plate in configuration 1, air passage only on the upper surface, and for configuration 2, air passage through the upper and lower surfaces one can conclude that the configuration 2 has better performance. The results show that configuration 2 is more suitable for drying products, with thermal efficiency of 19.8%, while configuration 1 obtained 8.4% for almost same conditions. The amount of moisture removed for configuration 1 was 185 g and for configuration 2 it was 266 g. The configuration 2 also recorded higher values for air flow, with an increase of 5.5%. Air temperature increases about 4.3% and the relative humidity inlet-outlet difference increases about 81.8%, when compared to configuration 1. Configuration 1 don't present any advantage over configuration 2.

Future studies will analyze configuration 2 with the integration of a thermal accumulator, using Phase Change Material (PCM) as a thermal storage. Changes in the location of the drying chamber aiming improvements in the amount of moisture removed will be also evaluated.

5. REFERENCES

Avallone, E., Mioralli, P.C., Scalon, V.L., Padilha, A. and Oliveira, S.D.R., 2018. "Thermal Pyranometer Using the Open Hardware Arduino Platform". *International Journal of Thermodynamics*, Vol. 21, No. 1, pp. 1–5. ISSN 1301-9724. doi:10.5541/ijot.5000209000. URL https://dergipark.org.tr/tr/pub/ijot/400063. Number: 1.

Baniasadi, E., Ranjbar, S. and Boostanipour, O., 2017. "Experimental investigation of the performance of a mixed-mode solar dryer with thermal energy storage". *Renewable Energy*, Vol. 112, pp. 143–150. ISSN 0960-1481. doi:10.1016/j.renene.2017.05.043. URL http://www.sciencedirect.com/science/article/pii/S0960148117304287.

Bell, I.H., Wronski, J., Quoilin, S. and Lemort, V., 2014. "Pure and pseudo-pure fluid thermophysical property evaluation and the open-source thermophysical property library coolprop". *Industrial & Engineering Chemistry Research*, Vol. 53, No. 6, pp. 2498–2508. doi:10.1021/ie4033999. URL http://pubs.acs.org/doi/abs/10.1021/ie4033999.

Mohajer, A., Nematollahi, O., Joybari, M.M., Hashemi, S.A. and Assari, M.R., 2013. "Experimental investigation of a Hybrid Solar Drier and Water Heater System". *Energy Conversion and Management*, Vol. 76, pp. 935–944. ISSN 0196-8904. doi:10.1016/j.enconman.2013.08.047. URL http://www.sciencedirect.com/science/article/pii/S0196890413005219.

Rajkumar, P., Kulanthaisami, S., Raghavan, G.S.V., Gariépy, Y. and Orsat, V., 2007. "Drying Kinetics of Tomato Slices in Vacuum Assisted Solar and Open Sun Drying Methods". *Drying Technology*, Vol. 25, No. 7-8, pp. 1349–1357. ISSN 0737-3937. doi:10.1080/07373930701438931. URL https://doi.org/10.1080/07373930701438931.

Singh, S. and Kumar, S., 2012. "Development of convective heat transfer correlations for common designs of solar dryer". *Energy Conversion and Management*, Vol. 64, pp. 403–414. ISSN 0196-8904. doi:10.1016/j.enconman.2012.06.017. URL http://www.sciencedirect.com/science/article/pii/S0196890412002804.